THE JOURNAL OF BIOLOGICAL CHEMISTRY VOL. 281, NO. 15, pp. 10206–10213, April 14, 2006

The Urokinase/PAI-2 Complex

*A NEW HIGH AFFINITY LIGAND FOR THE ENDOCYTOSIS RECEPTOR LOW DENSITY LIPOPROTEIN RECEPTOR-RELATED PROTEIN**[S]

Received for publication, December 22, 2005, and in revised form, January 17, 2006 Published, JBC Papers in Press, February 3, 2006, DOI 10.1074/jbc.M513645200

David Croucher[‡1], **Darren N. Saunders**[§2], **and Marie Ranson**[‡3]

From the [‡]*School of Biological Sciences, University of Wollongong, New South Wales 2522 and the* [§]*Cancer Research Program, Garvan Institute of Medical Research, Darlinghurst, New South Wales 2010, Australia*

The efficient inactivation of urokinase plasminogen activator (uPA) by plasminogen activator inhibitor type 2 (PAI-2) at the surface of carcinoma cells is followed by rapid endocytosis of the uPA-PAI-2 complex. We now show that one pathway of this receptor-mediated endocytosis is mediated via the low density lipoprotein receptor-related protein (LRP) in prostate cancer cells. Detailed biochemical analyses using ligand binding assays and surface plasmon resonance revealed a novel and distinct interaction mechanism between native, human LRP and uPA-PAI-2. As reported previously for PAI-1, inhibition of uPA by PAI-2 significantly increased the affinity of the complex for LRP (K_D of 36 nM for uPA-PAI-2 *versus* 200 nM for uPA). This interaction was maintained in the presence of uPAR, confirming the validity of this interaction at the cell surface. However, unlike PAI-1, no interaction was observed between LRP and PAI-2 in either the stressed or the relaxed conformation. This suggests that the uPA-PAI-2-LRP interaction is mediated by site(s) within the uPA molecule alone. Thus, as inhibition of uPA by PAI-2 resulted in accelerated clearance of uPA from the cell surface possibly via its increased affinity for LRP, this represents a mechanism through which PAI-2 can clear proteolytic activity from the cell surface. Furthermore, lack of a direct interaction between PAI-2 and LRP implies that downstream signaling events initiated by PAI-1 may not be activated by PAI-2.

Inhibition of urokinase plasminogen activator (uPA)[4] proteolytic activity at the cell surface is an important step in the regulation of pericellular plasminogen activation (1–4). This process is facilitated by members of the serpin (serine protease inhibitor) superfamily, most notably by plasminogen activator inhibitors 1 (PAI-1) and 2 (PAI-2) (SerpinE1 and SerpinB2, respectively) (5–7). Although both are efficient uPA inhibitors, PAI-1 and PAI-2 are structurally and functionally quite distinct serpins, as recognized by their grouping into different serpin subfamily groups (6). For example, PAI-1 also has alternative non-uPA inhibitory activities that affect cell adhesion, intracellular signaling, and cell migration (8) that have not been demonstrated for PAI-2.

In their classical inhibitory role, serpins interact with their target protease through an exposed peptide loop, the reactive center loop (6, 9). This acts as bait for the active site of the protease, leading to formation of an equimolar covalent complex. The formation of this complex results in extensive deformation of both the protease and the serpin (9), resulting in the conversion of the serpin from a "stressed" to a "relaxed" form. The relaxed conformation of PAI-2 and other serpins can also be induced by the insertion of a peptide that mimics the reactive center loop (10).

uPA is a potent marker of metastatic capacity in multiple human tumors and makes an attractive therapeutic target (11–13). Recent work has shown that cytotoxins attached to the PAI-2 molecule can be specifically delivered to malignant xenografts by targeting cell surface uPA (14–17), despite the apparent high levels of endogenous PAI-1 associated with malignant carcinoma (summarized in Ref. 12). Consequently, an understanding of the fate of uPA-bound PAI-2 not only addresses an under-characterized aspect of the plasminogen activation system but is fundamental to the development of PAI-2 as a cancer therapy.

We recently reported that the efficient and rapid inhibition of uPAR-bound uPA by PAI-2 at the surface of MDA-MB-231 and PC-3 carcinoma cells led to the rapid internalization of the uPAR/uPA-PAI-2 complex and delivery into endosomes and lysosomes (7). The internalization of PAI-2 was shown to be uPA-dependent and partially inhibited by the receptor-associated protein (RAP), an antagonist of ligand binding to members of the low density lipoprotein receptor (LDLR) family (18), indicating the involvement of LDLR family members in the receptor-mediated endocytosis of uPA-PAI-2. However, the mechanism(s) of endocytosis for PAI-2 are unknown.

The receptor-mediated endocytosis of uPA-PAI-1 complexes is known to be mediated by a high affinity interaction with at least three different members of the LDLR family of endocytosis receptors: the low density lipoprotein receptor-related protein (LRP, CD91) (19, 20), the very low density lipoprotein receptor (VLDLR) (21–23), and LRP-2 (megalin or gp330) (24). Following endocytosis, the uPA-PAI-1 complex is degraded in the lysosomes (25, 26), and uPAR is recycled back to the cell surface (27). All three interactions are inhibitable by RAP (18, 23) and are calcium-dependent as the conformation of the receptor is dependent upon the binding of calcium ions (18, 28). In terms of the endocytosis of serpin:uPA complexes, LRP is the most thoroughly characterized LDLR family member (19, 29–33). LRP binds and internalizes numerous, structurally diverse ligands and has been implicated in a range of biological processes including receptor endocytosis, cell signaling, antigen presentation, phagocytosis, and regulation of vascular permeability (reviewed in Ref. 34). LRP is a 600-kDa cell surface receptor,

* This work was funded in part by National Health and Medical Research Council Development Grant 213119. The costs of publication of this article were defrayed in part by the payment of page charges. This article must therefore be hereby marked "*advertisement*" in accordance with 18 U.S.C. Section 1734 solely to indicate this fact.

[S] The on-line version of this article (available at http://www.jbc.org) contains a supplemental figure.

[1] A Cancer Institute of New South Wales Research Scholar and recipient of an Australian Postgraduate Award. Supported by the Cancer Institute of New South Wales.

[2] Funded by a U. S. Department of Defense Breast Cancer Research Program Post-Doctoral Traineeship (Grant DAMD170310410).

[3] To whom correspondence should be addressed. Tel.: 61-2-4221-3291; Fax: 61-2-4221-4135; E-mail: mranson@uow.edu.Au.

[4] The abbreviations used are: uPA, urokinase plasminogen activator; uPAR, urokinase plasminogen activator receptor; serpin, serine protease inhibitor; HMW-uPA, high molecular weight uPA; LMW-uPA, low molecular weight uPA; LRP, low density lipoprotein receptor-related protein; PAI-1, plasminogen activator inhibitor type 1; PAI-2, plasminogen activator inhibitor type 2; RAP, receptor-associated protein; LDLR, low density lipoprotein receptor; VLDLR, very low density lipoprotein receptor; SPR, surface plasmon resonance; BSA, bovine serum albumin; FITC, fluorescein isothiocyanate; PBS, phosphate-buffered saline; TBS, Tris-buffered saline; TBST, TBS containing Tween 20; HRP, horseradish peroxidase.

comprised of an 85-kDa transmembrane domain and a 515-kDa extracellular domain (35). LRP has been identified within both clathrin-coated pits and caveolae/lipid rafts (34) and is proposed to regulate the protein composition of the plasma membrane, and hence, the interface between cells and the surrounding microenvironment.

Comprehensive analysis of the interaction between uPA-PAI-1, PAI-1, and LRP has previously been undertaken (36–39). This has not been the case for PAI-2, possibly as a result of a previous study using denatured bovine LRP that found no interaction between uPA-PAI-2 and LRP (40). Herein, we report for the first time that PAI-2 is internalized by a process of receptor-mediated endocytosis, and by using techniques that maintain the native, calcium-dependent conformation of human LRP, that this involves a high affinity interaction between uPA-PAI-2 and native LRP. Our results suggest that the high affinity binding sites for LRP lie solely within the uPA moiety of the uPA-PAI-2 complex as we could find no evidence of a corresponding site within either the relaxed or the stressed PAI-2 molecule. This indicates a clear distinction with PAI-1, in which a high affinity site within the PAI-1 moiety of uPA-PAI-1 complex contributes significantly to LRP binding (38). Furthermore, the uPA-PAI-2 complex is still able to bind LRP in the presence of uPAR, indicating the validity of this interaction at the cell surface. This has important physiological implications for pericellular proteolytic control.

EXPERIMENTAL PROCEDURES

Proteins, Antibodies, and Reagents—Recombinant human PAI-2 (47-kDa form) and PAI-2 CD loop mutant (residues 66–98 deleted) (41) were provided by PAI-2 Proprietary Ltd. (Sydney, Australia). Purified human placental LRP was a kind gift from Prof. Phillip Hogg (University of New South Wales, Sydney, Australia). Active human uPA HMW/LMW mixture was from Chemicon. Human HMW uPA was from American Diagnostica. Purified human RAP and rabbit anti-LRP polyclonal antibody were a kind gift from Prof. Dudley Strickland (American Red Cross). Anti-LRP light chain (catalog number 3501), PAI-2 (catalog number 3750), and anti-uPA (catalog number 394) monoclonal antibodies were from American Diagnostica. Anti-VLDLR (H-95) and anti-LRP2 (H-245) polyclonal antibodies were from Santa Cruz Biotechnology (Santa Cruz, CA). Recombinant human uPAR was from Calbiochem. Anti-DNP rabbit polyclonal isotype control was from DakoCytomation (Glostrup, Denmark). Transferrin:Alexa Fluor 488 was a kind gift from Dr. Ellen Van Dam (Garvan Institute, Sydney, Australia). The Alexa Fluor 488 labeling kit and Alexa Fluor 488 polyclonal antibody were from Molecular Probes. PD-10 columns were obtained from Amersham Biosciences. Biotin NHS and enhanced chemiluminescence kit were from Pierce. Mono-C ion exchange spin columns were from Sartorius (Goettingen, Germany). 30-kDa cut-off protein concentration spin columns were from Millipore. BIAcore CM5 chips and amine linking kit were from BIAcore (Melbourne, Australia). Bovine serum albumin (BSA), propidium iodide, Hanks' balanced salts powder, EDTA, streptavidin-FITC, Goat anti-mouse IgG-FITC, Goat anti-rabbit IgG-FITC, chlorpromazine, and nystatin were from Sigma. Neutravidin-HRP, reagents for SDS-PAGE, and broad range unstained molecular weight marker were from Bio-Rad Laboratories, (Sydney, Australia). RPMI 1640 powder and fetal calf serum were from Trace Bioscientific (Melbourne, Australia).

Tissue Culture Conditions—The PC-3 epithelial prostate cancer cell line was used for all experiments. Cells were grown, passaged, and prepared for experiments as described previously (7). Briefly, cells were cultured for 48 h without a change of medium and were detached using PBS/EDTA (5 mM) either prior to or during the experiment, as described. All cell experiments were conducted in binding buffer (phenol red-free Hanks' buffered salt solution, pH 7.4, containing 1 mM $CaCl_2$, 1 mM $MgCl_2$, and 0.1% BSA).

Fluorescence Quenching Internalization Assay—Internalization assays were undertaken essentially as described previously (7) and adapted for use with attached cells. Briefly, PC-3 cells grown in a 6-well plate to subconfluency over a 48-h period were washed once with 1 ml of binding buffer and then incubated for 1 h at 37 °C in binding buffer to precycle cell surface receptors. The cells were preincubated for 10 min with RAP (100 nM), anti-LRP polyclonal antibody (50 μg/ml), anti-DNP irrelevant isotype (50 μg/ml), anti-uPA monoclonal antibody (20 μg/ml), chlorpromazine (30 μM), or nystatin (20 μM) at 37 °C or combinations of these as indicated. The Alexa Fluor 488-labeled protein of interest was then added to a concentration of 10 nM, and the cells were incubated at 37 °C for the time period indicated. Following this, the cell monolayers were washed twice with ice-cold binding buffer, detached with PBS/EDTA (5 mM) for 3 min at room temperature, and resuspended at 2×10^6/ml in ice-cold binding buffer. The cells were then incubated in the presence of 4 μg/ml anti-Alexa Fluor 488 polyclonal antibody for 30 min on ice.

After this incubation period, the cells were centrifuged at $300 \times g$ at 4 °C, resuspended in ice-cold PBS containing the vital fluorescent stain propidium iodide (1 μg/ml), and analyzed by dual color flow cytometry as described previously (42). Cells not incubated with Alexa Fluor 488-labeled proteins, but subjected to the same treatments, were used as a measure of autofluorescence. The mean value of two autofluorescence samples was calculated and subtracted from all relevant values. A control experiment to determine the effects of nystatin on clathrin-dependent internalization was undertaken in the same manner using transferrin:Alexa Fluor 488 as the internalized ligand.

Measurement of Cell Surface Endogenous Receptor Expression by Flow Cytometry—PC-3 cells, grown to subconfluency over a 48-h period, were detached using PBS/EDTA (5 mM), washed with ice-cold binding buffer, and centrifuged at $300 \times g$ at 4 °C. The cells were resuspended at 1×10^6 cells/ml in ice-cold binding buffer containing primary polyclonal antibodies or their irrelevant isotype control antibody (5 μg/ml) or biotinylated RAP (10 nM) and incubated for 45 min on ice. Proteins were biotin-labeled using biotin NHS according to the manufacturer's instructions. After three washes with ice-cold binding buffer, the cells were incubated with goat anti-rabbit IgG-FITC (1:50 dilution) or streptavidin-FITC (1:200 dilution), respectively, for 45 min on ice. In all cases, cell surface fluorescence was analyzed by dual color flow cytometry as described previously (42).

Co-localization Studies Using Confocal Microscopy—Confocal fluorescence microscopy was performed essentially as described previously (43), with the exception of the PAI-2 binding and internalization step. Briefly, PC-3 cells were grown on glass coverslips, washed with ice-cold binding buffer, and preincubated for 1 h in binding buffer at 37 °C to precycle cell surface receptors. Following this, the cell monolayers were incubated with 10 nM preformed biotinylated PAI-2-streptavidin-FITC complex for 1 h at 18 °C. After a further washing with ice-cold PBS, the cells were fixed with 3.75% paraformaldehyde for 20 min on ice. The cells were permeabilized using 0.2% Triton-X100 in PBS for 5 min at room temperature, washed with ice-cold PBS, and nonspecific sites were blocked by incubation with PBS/BSA (0.1%) for 30 min on ice. LRP was detected by incubation with 10 μg/ml anti-LRP polyclonal antibody in PBS/BSA (0.1%) for 45 min on ice. After two washes with ice-cold PBS, the cells were incubated with goat anti-rabbit IgG-Cy5 (1:50 dilution) and TOPRO nuclear counterstain (1:400) in PBS/BSA (0.1%) for 45

min on ice. After two washes, the cells were analyzed by confocal microscopy using a Leica TCS SP system (Leica, Heidlberg, Germany).

Binding of uPA-PAI-2 to Immobilized LRP—Ligand blotting was undertaken for the initial characterization of uPA-PAI-2 binding to LRP as this procedure is often used to investigate the interaction between LRP and potential ligands (39, 44, 45). Purified LRP (1 μg) was dotted onto nitrocellulose and dried for 30 min at 37 °C. The membrane was then blocked by incubation in Tris-buffered saline containing Tween 20 (0.05%) (TBST) and 3% gelatin for 1 h at room temperature. After three 10-min washes with TBST/$CaCl_2$ (1 mM), the membranes were incubated with various biotinylated ligands or monoclonal antibodies for 1 h at room temperature in TBST, 1% gelatin, $CaCl_2$. We have previously demonstrated that incubation of an equimolar ratio of uPA to PAI-2 results in almost complete inactivation of uPA by conversion to uPA-PAI-2 complex (46). Hence, complexes between uPA and biotinylated PAI-2 were formed by incubating a 10 M excess of PAI-2 with uPA at 37 °C for 90 min to facilitate maximal formation of uPA-PAI-2 complexes while minimizing formation of cleavage products from excess uPA (data not shown). In some cases, the membranes were preincubated with RAP (100 nM) or EDTA (5 mM) in TBST, 1% gelatin, $CaCl_2$ for 30 min at room temperature and then washed prior to adding ligands or antibodies. In the case of EDTA inhibition, EDTA (5 mM) was also present during the incubation with uPA-PAI-2 to prevent the restoration of calcium binding by LRP. After another three 10-min washes with TBST, the membranes were incubated with neutravidin-HRP (1:10,000 dilution) or rabbit anti-mouse IgG-HRP (1:50 dilution) for 1 h at room temperature in TBST, 1% gelatin, $CaCl_2$. Following a further three 10-min washes with TBST/$CaCl_2$, the membranes were finally washed with TBS for 10 min and then developed by enhanced chemiluminescence.

Surface Plasmon Resonance Analysis—To further analyze the interaction between uPA-PAI-2 complex and LRP, surface plasmon resonance (SPR) assays were performed using a BIAcore 2000 (BIAcore AB, Uppsala, Sweden). To prepare HMW and LMW uPA-PAI-2 complexes, a 10-fold M excess of PAI-2 was incubated with a mixture of HMW and LMW uPA for 90 min at 37 °C. The crude mixture of uPA-PAI-2 complexes was buffer-exchanged into 50 mM phosphate buffer (pH 6) using 30-kDa cut-off spin columns. The crude mixture was applied to a mono-C ion-exchange spin column that was centrifuged at 300 × *g* for 4 min. Following three 400-μl washes with 50 mM phosphate buffer, the bound proteins were eluted using a NaCl step gradient (0–1 M) by applying 400-μl aliquots of increasing NaCl concentration to the column between each centrifugation and elution step (46). Non-reducing SDS-PAGE confirmed the presence of purified uPA-PAI-2 complexes.

Relaxed PAI-2 was formed by the incubation of PAI-2 (1 mg/ml) with a 10-fold M excess of reactive center loop peptide in 10 mM phosphate buffer (pH 8) for 48 h at 37 °C. Excess reactive center loop peptide was removed using a 30-kDa cut-off spin column. The extent of relaxed PAI-2 formation was determined by incubating PAI-2 with uPA (5:1 M ratio) for 90 min at 37 °C and determining complex formation using SDS-PAGE. This method has previously been shown to result in complete conversion of PAI-2 to the relaxed conformation, forming stable PAI-2/reactive center loop complex with no detectable uPA-inhibitory activity (10, 46).

LRP was immobilized to a CM5 BIAcore chip according to the manufacturer's instructions. Briefly, the chip was activated using a 1:1 mixture of 0.2 M *N*-ethyl-*N*′-(3-dimethylaminopropyl)carbodiimide and 0.05 M *N*-hydroxysuccimide. LRP was coated to the chip at 40 μg/ml in 10 mM sodium acetate (pH 3) for 7 min at 5 μl/min, as described previously (39). The immobilization resulted in LRP coated to the chip between 15–28 fmol/mm^2. The unoccupied binding sites were blocked using 1 M ethanolamine, pH 8.5. Ligands were desalted into running buffer (HEPES (10 mM) pH 7.4, NaCl (140 mM), $CaCl_2$ (1 mM) and 0.05% Tween 20) before applying to the BIAcore chip at 20 μl/min. Regeneration of the chip was achieved using 1.6 M glycine (pH 3), EDTA (5 mM). All buffers were filtered and degassed before use. For kinetic analysis, a blank cell was used as the reference cell, and data were analyzed using BIAevaluation software (Version 4). A one-binding site model with a drifting baseline provided the best fit according to χ^2 values and analysis of residual plots.

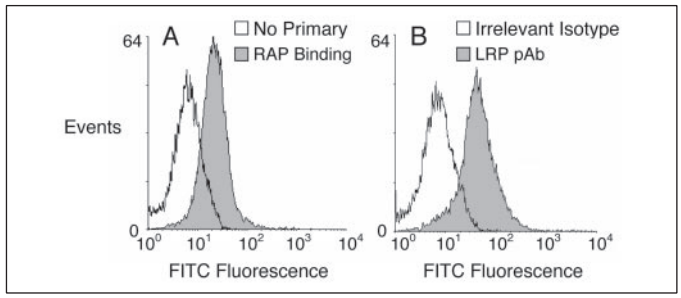

FIGURE 1. **LRP is expressed on PC-3 cells.** The cells were probed with biotinylated RAP (100 nM) (*A*) and a polyclonal antibody to LRP (5 μg/ml) (*B*). These were detected with streptavidin-FITC and goat anti-rabbit IgG-FITC, respectively, and analyzed by flow cytometry, using propidium iodide to exclude non-viable cells.

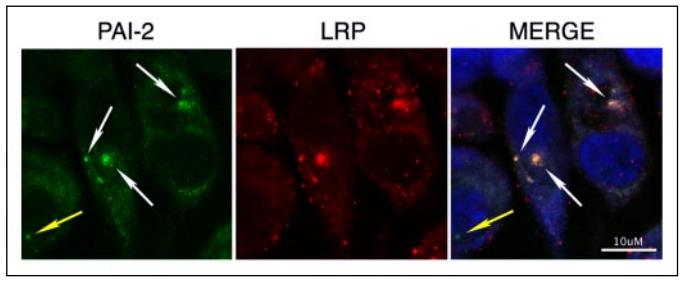

FIGURE 2. **Co-localization of internalized PAI-2 and LRP.** PC-3 cells were washed with ice-cold binding buffer and incubated at 37 °C for 1 h to precycle cell surface receptors. Following this, the cells were incubated with 10 nM preformed biotinylated PAI-2/streptavidin-FITC complex for 1 h at 18 °C. Cells were washed with ice-cold binding buffer, fixed with 3.75% paraformaldehyde, and permeabilized with 0.2% Triton X-100. After incubation with 10 μg/ml anti-LRP polyclonal antibody, the cells were washed and incubated with goat anti-rabbit IgG-Cy5 (1:50 dilution) and TOPRO (1:400). After washing, the cells were analyzed by immunofluorescence and confocal microscopy for LRP (*red*) and PAI-2 (*green*). Co-localized PAI-2 and LRP (indicated by *white arrows*) is represented by *yellow* in the merged image. *Yellow arrows* show PAI-2 that was not co-localized with LRP. *Scale bars* are 10 μm.

RESULTS

Candidate Endocytosis Receptors Involved in the Internalization of PAI-2—We have previously shown efficient inhibition of cell surface uPA by PAI-2 on carcinoma cell lines followed by rapid internalization of the uPAR/uPA-PAI-2 complex and delivery into endosomes and lysosomes through a RAP-inhibitable mechanism (7), suggesting internalization via receptor-mediated endocytosis. The binding of biotinylated RAP to PC-3 cells (Fig. 1*A*) indicated the presence of receptors from the LDLR family at the cell surface. Further analysis indicated that LRP was expressed at the surface of PC-3 cells, as detected by flow cytometry (Fig. 1*B*), and a proportion of the internalized PAI-2 was observed to co-localize with LRP in intracellular vesicles (Fig. 2). This was confirmed to be RAP-sensitive as little or no co-localized PAI-2 and LRP could be detected in the presence of RAP by confocal microscopy (data not shown). VLDLR was barely detectable, and megalin (LRP-2) was not detectable on these cells as determined by flow cytometry (data not shown). We then employed a number of established endocytosis

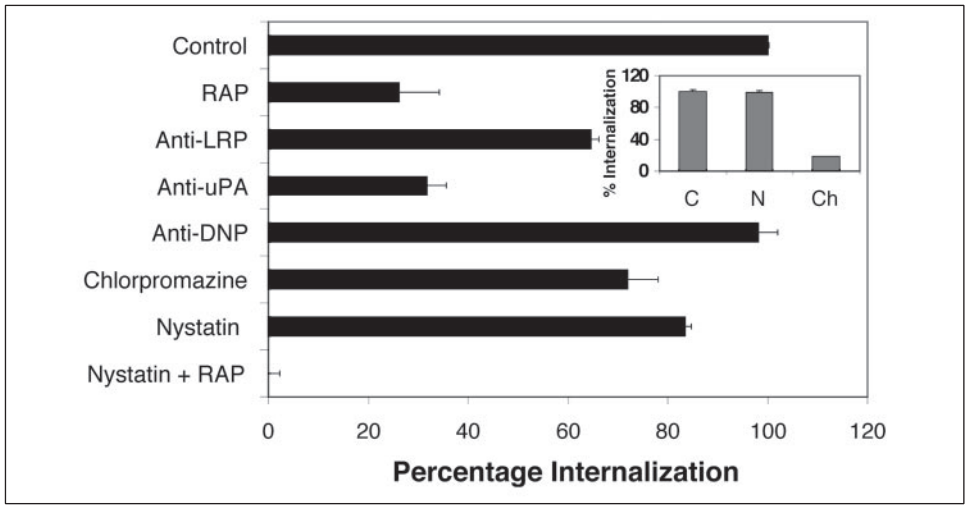

FIGURE 3. **PAI-2 endocytosis can be prevented by inhibitors of clathrin-dependent and -independent processes.** PC-3 cells were treated with RAP (200 nM), anti-LRP polyclonal antibody (50 μg/ml), anti-uPA monoclonal antibody (20 μg/ml), anti-DNP polyclonal antibody (50 μg/ml), chlorpromazine (30 μM), or nystatin (20 μM) for 10 min at 37 °C or a combination of these as indicated, prior to analysis of PAI-2:Alexa Fluor 488 internalization by the fluorescence quenching internalization assay. Chlorpromazine and nystatin were used at subtoxic doses (cell viability over 70%) as determined by propidium iodide exclusion and dual color flow cytometry (data not shown). Each value for internalized PAI-2/transferrin was taken as a percentage of the relevant control (values are ± S.E., $n = 3$). Values obtained for all treatments, except the anti-DNP irrelevant isotype, are significantly different to the control ($p < 0.05$). *Inset*, inhibition of transferrin:Alexa Fluor 488 endocytosis was used as a positive control for chlorpromazine (*Ch*) activity (57) and to confirm a lack of effect by nystatin (*N*) on a clathrin-dependent process as compared with control (*C*).

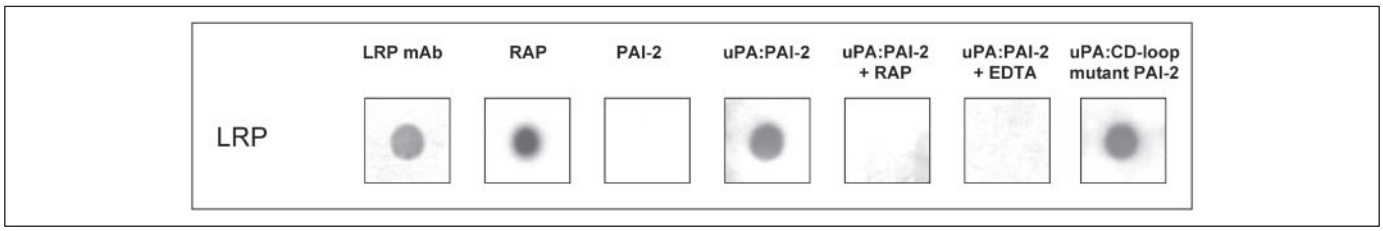

FIGURE 4. **Ligand dot blot analysis of the interaction between uPA-PAI-2 and LRP.** Immobilized LRP (1 μg) was incubated with various biotinylated ligands or monoclonal antibodies (*mAb*) (as shown). For RAP and EDTA inhibition of uPA-PAI-2 binding, membranes were preincubated with RAP (100 nM) or EDTA (5 mM). Biotinylated ligands were detected with neutravidin-HRP (1:10,000 dilution) and monoclonal antibodies with rabbit anti-mouse IgG-HRP (1:50 dilution).

inhibitors to further characterize the mechanism(s) of PAI-2 endocytosis (Fig. 3). As shown previously, PAI-2 endocytosis is substantially inhibited by either RAP (7) or anti-catalytic uPA antibody (~75% of control), confirming that the majority of PAI-2 internalization is both uPA-dependent and mediated by the LDLR family of receptors. The anti-catalytic uPA antibody is known to efficiently inhibit PAI-2 binding to cell surface uPA (7). Incomplete inhibition of internalization by this antibody may represent either nonspecific fluid phase take-up of PAI-2 or an alternative (*i.e.* uPA-independent) binding site for PAI-2 on the cell surface of PC-3 cells.

Preincubation with a polyclonal antibody against LRP, previously used to inhibit endocytosis of LRP ligands (24), resulted in ~40% inhibition of PAI-2 endocytosis (Fig. 3). This may indicate inefficient inhibition by the anti-LRP polyclonal antibody, or alternately, that the remaining 20–30% of RAP-dependent endocytosis of PAI-2 may be mediated by VLDLR. Chlorpromazine, an inhibitor of the formation of clathrin lattices, and nystatin, a cholesterol-sequestering agent that breaks down caveolae and lipid rafts (47), inhibited ~25 and ~20% of PAI-2 endocytosis, respectively (Fig. 3). Critically, the addition of both nystatin and RAP resulted in a complete inhibition of PAI-2 endocytosis (Fig. 3). Taken together, these data indicate that a small but significant component of PAI-2 endocytosis is mediated by a uPA- and LDLR family member-independent mechanism(s). Nevertheless, LRP clearly facilitates a significant proportion of PAI-2 endocytosis in PC-3 cells.

The Interaction between uPA-PAI-2 and LRP—As there are no existing data pertaining to the potential interaction of uPA-PAI-2 with LRP, we undertook studies to examine the biochemical interactions underlying this mechanism. Initial characterization of the interaction between uPA-PAI-2 and LRP was undertaken via ligand blotting (Fig. 4). This analysis showed a direct interaction between uPA-PAI-2 complex and LRP; however, no interaction between PAI-2 alone and LRP was detected. The uPA-PAI-2/LRP interaction was inhibited by preincubation with either RAP or EDTA, indicating specific, calcium-dependent binding. Deletion of the CD loop within PAI-2 (41) did not affect binding of uPA-PAI-2 to LRP.

SPR analysis was undertaken to obtain a more detailed analysis of uPA-PAI-2 binding to LRP (Fig. 5 and Table 1). In support of the ligand blotting data, no interaction between LRP and PAI-2 (in either the stressed or the relaxed conformation) was detected (Fig. 5). A high affinity interaction, which best fit a one-binding site model, was observed between uPA-PAI-2 and LRP (K_d ~36 nM) (Table 1). HMW uPA also bound LRP with a one-binding site model, although with ~5.5-fold lower affinity (K_d ~200 nM). No interaction was observed between LRP and a complex of LMW uPA (*i.e.* uPA lacking the amino-terminal fragment region, 33 kDa) and PAI-2 (Fig. 5).

Detailed analysis of SPR data for uPA and uPA-PAI-2 binding to LRP revealed that the rate of dissociation of uPA from LRP was not significantly altered upon PAI-2 inhibition (Table 1). However, the rate of association of uPA-PAI-2 with LRP was increased ~8-fold as compared with the rate of uPA association.

The increase in affinity of uPA-PAI-2 for LRP was also reflected in the enhanced clearance of uPA from the cell surface. For example, uPA was internalized by PC-3 cells with a $t_{½}$ of ~100 min, whereas uPA-PAI-2 was internalized with a $t_{½}$ of ~20 min (R^2 values of 0.94 and 0.95, respectively) (Fig. 6). These data also confirm our previous observations, using different techniques, of slow constitutive cell surface uPA turnover in the absence of inhibitors (7).

Effect of uPAR on uPA-PAI-2 Binding to LRP—uPA is bound to the cell surface via its receptor uPAR; hence, *in vivo* interactions between uPA-PAI-2 and LRP are likely to occur in close proximity to, and may be regulated, by uPAR. Using SPR analysis, uPAR-bound uPA was observed to interact with LRP. Significantly, formation of serpin:pro-

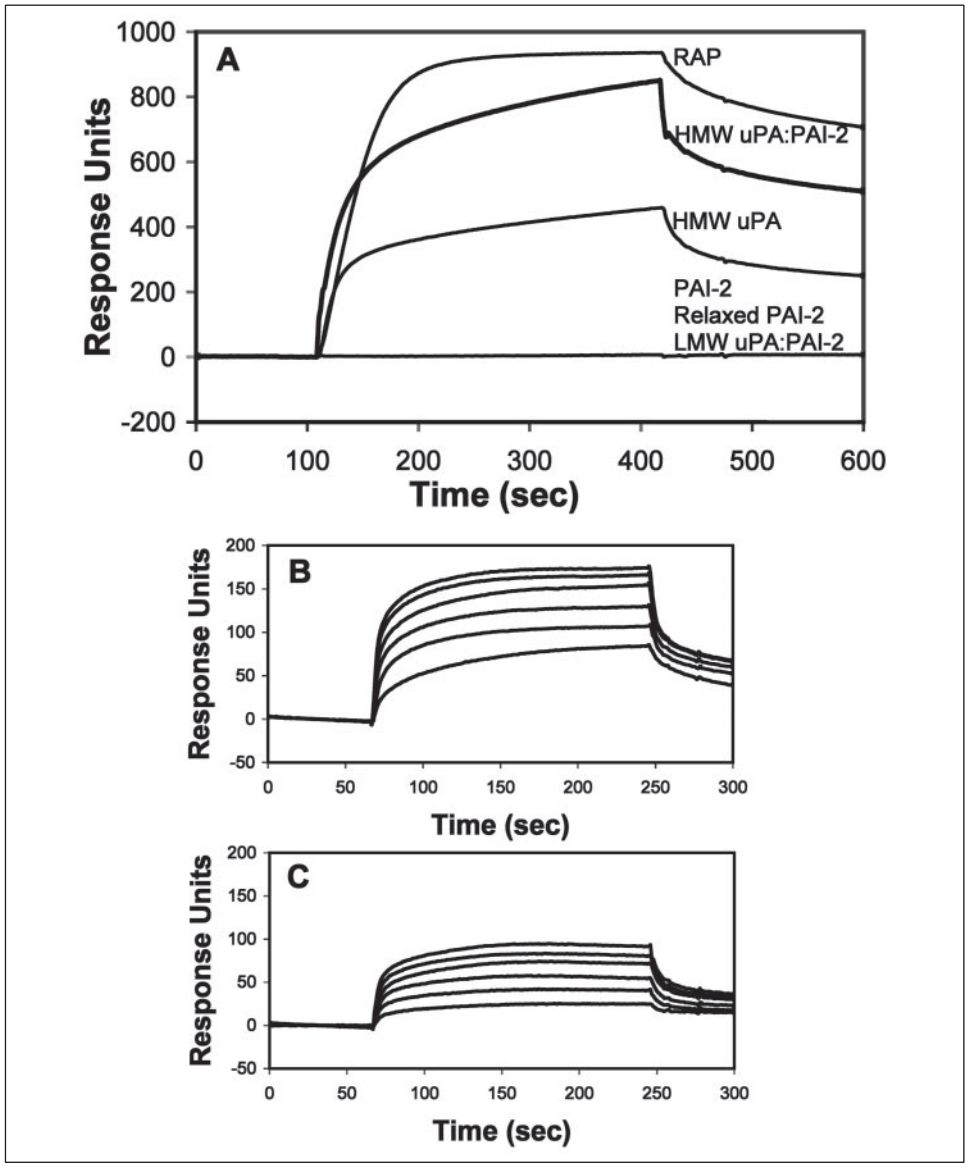

FIGURE 5. **Surface plasmon resonance analysis of the interaction between uPA-PAI-2 and LRP.** *A*, sensorgrams showing the interaction between 100 nM stressed PAI-2, relaxed PAI-2, HMW uPA, HMW uPA-PAI-2, LMW uPA-PAI-2, and immobilized LRP. RAP (100 nM) was used as a positive control. The data shown are representative of at least three independent experiments. *B*, sensorgram showing the dose-dependent binding of uPA-PAI-2 (25–150 nM) to LRP. *C*, sensorgram showing the dose-dependent binding of uPA (100–600 nM) to LRP.

tease complex (*i.e.* uPA-PAI-2) in the presence of saturating amounts of uPAR resulted in a significant increase in binding to LRP as compared with uPA alone (Fig. 7*A*). It should be noted that binding of both uPA and uPA-PAI-2 to LRP is reduced in the presence of uPAR as compared with free ligands. Using both enzyme-linked immunosorbent assay (data not shown) and SPR techniques (Fig. 7*B*), no interaction between uPAR and LRP was found, confirming the lack of a binding site on uPAR for LRP (36).

DISCUSSION

The efficient inactivation of uPA by PAI-2 at the surface of carcinoma cells is followed by rapid internalization of the uPA-PAI-2 complex into endosomes and lysosomes (7). Herein we present definitive data showing that the majority of PAI-2 internalization is uPA-dependent and RAP-sensitive and that the resulting uPA-PAI-2 complex is a novel, high affinity ligand for LRP. This interaction is responsible in part for the receptor-mediated endocytosis of uPA-PAI-2/uPAR and the subsequent clearance of active uPA from the cell surface.

Several lines of evidence implicate LRP as an endocytosis receptor for uPA-PAI-2. Internalized PAI-2 co-localized with LRP, preincubation with anti-LRP polyclonal antibodies significantly inhibited PAI-2 endocytosis, and uPA-PAI-2 bound to LRP with high affinity. Hence, similar to other serpins, PAI-2 endocytosis can be mediated via LRP. As inhibition by an anti-LRP polyclonal antibody did not reflect the total amount of RAP inhibition, it is possible that VLDLR may also be involved in mediating the endocytosis of PAI-2. The role of this receptor in uPA-PAI-2 endocytosis, in this and other cell lines, is currently under further investigation.

As preincubation with either RAP or the anti-uPA antibody was unable to completely inhibit PAI-2 internalization, the presence of an alternative (*i.e.* uPA- and LRP-independent) PAI-2 binding site is possible. Inhibition of PAI-2 internalization by nystatin, a cholesterol-sequestering agent that breaks down membrane domains known to be involved in clathrin-independent endocytosis (primarily lipid rafts and caveolae) (47), strongly suggests the involvement of lipid rafts and/or caveolae in PAI-2 endocytosis. LRP has been detected within caveolae and lipid rafts (48, 49), suggesting that nystatin treatment may also interfere with LRP-dependent endocytosis of PAI-2. Indeed, we have detected LDLR family members in caveolae (detergent-resistant membrane fraction) extracted from PC-3 cells (data not shown). Further-

TABLE 1
The kinetics parameters of uPA and uPA:PAI-2 binding to LRP, measured by surface plasmon resonance

Analyte	k_{off}	k_{on}	K_d[a]	χ^2
	s^{-1}	$M^{-1}\,s^{-1}$	M	
uPA	7.78×10^{-3} ($\pm 1.31 \times 10^{-3}$)	3.87×10^{4} ($\pm 0.096 \times 10^{4}$)	2.00×10^{-7} ($\pm 0.29 \times 10^{-7}$)	0.45 ($\pm$0.118)
uPA:PAI-2	6.63×10^{-3} ($\pm 0.902 \times 10^{-3}$)	3.12×10^{5}[b] ($\pm 1.31 \times 10^{5}$)	3.62×10^{-8}[b] ($\pm 1.94 \times 10^{-8}$)	1.59 ($\pm$0.69)

[a] The binding data was fitted using the BIAevaluation 4.0 software. A one site binding model with a drifting baseline yielded the best fit for both analytes (lowest χ^2 value). (Values are the average result of three experiments, values are $\pm$ S.E.).
[b] Kinetic parameters for uPA:PAI-2 that were significantly different to those obtained for uPA ($p < 0.05$).

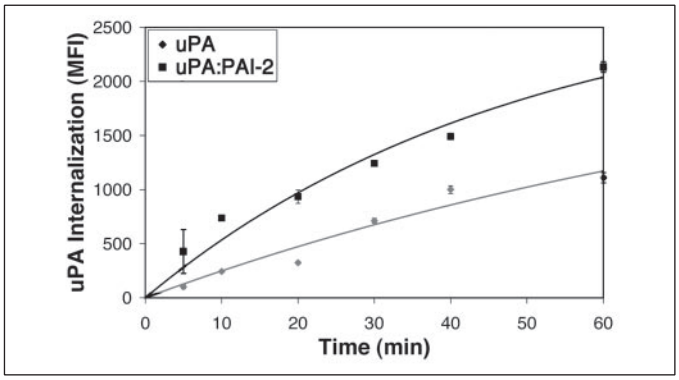

FIGURE 6. **Inhibition of uPA by PAI-2 results in enhanced clearance of the uPA-PAI-2 complex.** PC-3 cell monolayers, known to have up to 50% unoccupied uPAR (7), were incubated with 10 nM uPA:Alexa Fluor 488 or uPA:Alexa Fluor 488 complexed with PAI-2, at 37 °C for the time periods indicated. Cells were then analyzed using the fluorescence quenching internalization assay (values are $\pm$ S.E., $n = 3$). The mean fluorescence intensity (*MFI*) was calculated for values of internalized uPA.

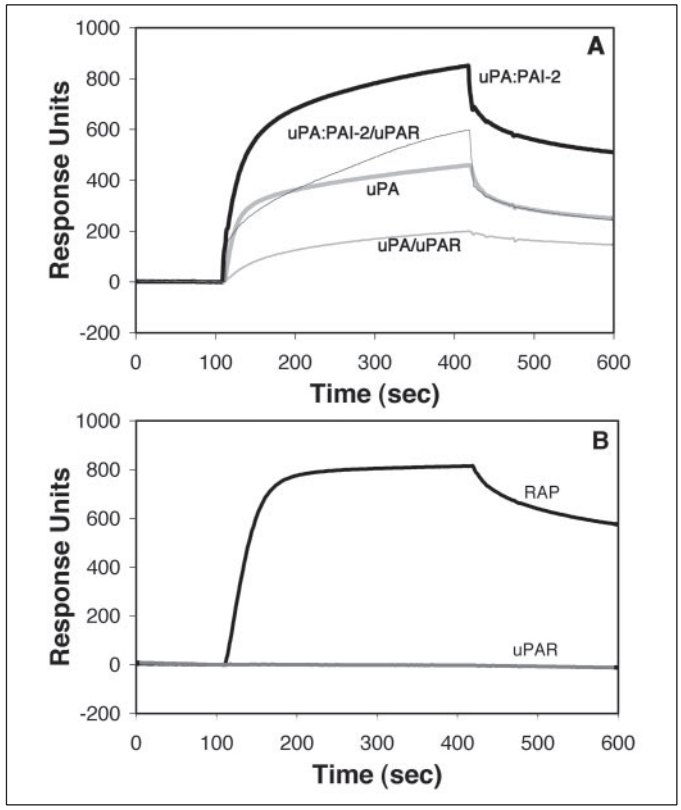

FIGURE 7. **Ligation to uPAR reduces the binding of both uPA and uPA-PAI-2 to LRP.** *A*, surface plasmon resonance sensorgrams of the binding of uPA (*gray lines*) and uPA-PAI-2 (*black lines*) to LRP in the presence (*thin lines*) and absence (thick lines) of a 10-fold M excess of uPAR. *B*, sensorgrams showing the lack of a direct interaction between uPAR (100 nm) (*gray line*) and LRP. RAP (100 nM) (*black line*) was used as a positive control for LRP binding.

more, the presence of LDLR family members within caveolae may also explain the persistence of uPA-PAI-2 internalization in the presence of chlorpromazine, whereas transferrin internalization (which is not mediated by receptors of the LDLR family) was almost completely inhibited. uPAR-dependent endocytosis of uPA-PAI-2 by caveolae is also not unfeasible as uPAR is known to localize into these regions (50). However, given that in the presence of both nystatin and RAP, PAI-2 internalization was completely abolished, an additional unknown uPA- and LDLR-independent mechanism of PAI-2 internalization mediated via caveolae or lipid rafts must also be operating in these cells.

Relatively high concentrations of free PAI-1 (active, latent, and cleaved) are able to compete for uPA-PAI-1 binding to LRP (36), and free PAI-1 can bind directly LRP independent of uPA (K_d ~93 nM) (8). However, we observed no interaction between stressed or relaxed PAI-2 (discussed further below) and LRP by either SPR or ligand dot blotting. SPR analysis revealed a low affinity interaction between HMW uPA and LRP (K_d ~200 nM), in agreement with previous studies (20). Critically, inhibition of uPA by PAI-2 and concomitant formation of uPA-PAI-2 complex resulted in a ~5.5-fold increase in affinity for LRP (K_d ~36 nM). This may explain in part the enhanced clearance of PAI-2-inhibited uPA observed in both PC-3 (Fig. 6) and MDA-MB-231 (7) cells, as shown for uPA-PAI-1 complexes in other cell lines (51). This in turn facilitates the clearance of cell surface plasminogen-activating capability (52) and may possibly mediate cell signaling events (53).

As binding sites for LRP exist in both the uPA and the PAI-1 moieties within the uPA-PAI-1 complex, this may account for the 12-fold higher affinity binding of uPA-PAI-1 to LRP (K_d ~3 nM) (20) as compared with that of uPA-PAI-2 to LRP. It is thought that the high affinity binding of uPA-PAI-1 to LRP results from either the combination of low affinity sites in each molecule (36) or the unveiling of a cryptic high affinity binding site within PAI-1 (38). Using synthetic reactive center loop peptides to induce the relaxed conformation of PAI-2 in the absence of uPA (thus mimicking that found in uPA-PAI-2 complex) (46), we found no evidence for an LRP binding site within PAI-2. Furthermore, there was no LRP binding by LMW uPA-PAI-2, which lacks the amino-terminal fragment of uPA, whereas LMW uPA-PAI-1 does bind to LRP (38). Hence, PAI-2 appears to be unique among protease:serpin complexes (36, 51) in lacking an LRP binding determinant. Considering the lack of significant change in dissociation rates between uPA/uPA-PAI-2 and LRP and the marked increase in the association rate of uPA-PAI-2 with LRP as compared with free uPA, it is likely that the same site within uPA is responsible for binding to LRP in the free and inhibited molecule. This site within uPA may become more available for LRP binding after the deformation induced by PAI-2 inhibition (possibly reducing steric hindrance to this site), hence increasing the association rate of uPA-PAI-2 for LRP.

The absence of a high affinity LRP binding site within the PAI-2 moiety has direct implications for cell signaling events mediated upon binding to LDLR family members by other serpins. For example, sustained extracellular signal-regulated kinase (ERK) phosphorylation and subsequent promotion of cell proliferation and migration depends on

the high affinity site within the PAI-1 moiety of uPA-PAI-1 binding to the VLDLR on MCF-7 cells (54). Furthermore, the ability of PAI-1 to bind LRP independently of uPA contributes to activation of the Jak/Stat pathway and stimulates cell migration (8). These data suggest the intriguing possibility that PAI-2 may be able to inhibit and clear cell surface uPA and therefore inhibit plasminogen activation ability, without initiating cell signaling events associated with metastatic potential. If proven, these effects may also partially explain the disparate relationships between PAI-1 and PAI-2 expression and disease outcome in various cancers, as it has been reported that high tumor PAI-2 antigen is related to a favorable overall survival (11, 55), whereas high PAI-1 antigen is related to a negative outcome (11, 12).

Importantly, we have shown that the increased binding of uPA-PAI-2 to LRP as compared with uPA is maintained in the presence of uPAR, although overall binding is reduced. The reduction in binding of uPA-PAI-2 to LRP upon uPAR binding is consistent with the findings of Nykjaer *et al.* (36), who showed that the binding of uPA-PAI-1 to LRP was significantly decreased in the presence of uPAR and that pro-uPA binding was entirely inhibited. This lowered affinity is most likely due to uPAR hindering the access of LRP to binding sites within the active uPA molecule. Regardless, these data indicate that the enhanced endocytosis of uPA-PAI-2 by LRP is relevant in the cell surface context, where uPA is bound to uPAR. Incidentally, we found no evidence of a direct interaction between uPAR and LRP. Although this is consistent with the findings of Nykjaer *et al.* (36), it conflicts with the findings of Czekay *et al.* (56), who suggested that uPAR binds to LRP independent of uPA-PAI-1 through a binding site in domain three of uPAR. This discrepancy may be explained by the different techniques used in these studies.

In conclusion, we present a mechanism of PAI-2 internalization by receptor-mediated endocytosis involving LRP following inhibition of uPAR-bound uPA. We show that the interaction between LRP and uPA-PAI-2 is most likely mediated by site(s) on the uPA molecule interacting with LRP. This interaction was maintained in the presence of uPAR, confirming the validity of this interaction at the cell surface. Significantly, in contrast to PAI-1, no interaction was observed between either stressed or relaxed PAI-2 and LRP. These findings have important implications for understanding the initiation of downstream cell signaling events mediated upon PAI-1 binding to LDLR family members and their potential role in metastasis. The rapid, LRP-mediated endocytosis of PAI-2 upon inhibition of cell surface uPA further validates the use of PAI-2 as an anti-uPA targeting strategy in cancer therapy. It also presents an avenue for intracellular delivery of toxins to cancer cells, increasing specificity and also efficacy of PAI-2 cancer therapies. Further studies will aim to investigate other LDLR- and non-LDLR-mediated endocytosis pathways for PAI-2 and determine the extent of caveolae/lipid raft involvement in this process.

Acknowledgment—BIAcore equipment was funded by Wellcome Trust Grant 052458.

REFERENCES

1. Cubellis, M. V., Andreasen, P., Ragno, P., Mayer, M., Dano, K., and Blasi, F. (1989) *Proc. Natl. Acad. Sci. U. S. A.* **86,** 4828–4832
2. Ellis, V., Wun, T. C., Behrendt, N., Ronne, E., and Dano, K. (1990) *J. Biol. Chem.* **265,** 9904–9908
3. Estreicher, A., Muhlhauser, J., Carpentier, J. L., Orci, L., and Vassalli, J. D. (1990) *J. Cell Biol.* **111,** 783–792
4. Pollanen, J., Vaheri, A., Tapiovaara, H., Riley, E., Bertram, K., Woodrow, G., and Stephens, R. W. (1990) *Proc. Natl. Acad. Sci. U. S. A.* **87,** 2230–2234
5. Kruithof, E., Baker, M., and Bunn, C. (1995) *Blood.* **86,** 4007–4024
6. Silverman, G. A., Bird, P. I., Carrell, R. W., Church, F. C., Coughlin, P. B., Gettins, P. G. W., Irving, J. A., Lomas, D. A., Luke, C. J., Moyer, R. W., Pemberton, P. A., Remold-O'Donnell, E., Salvesen, G. S., Travis, J., and Whisstock, J. C. (2001) *J. Biol. Chem.* **276,** 33293–33296
7. Al Ejeh, F., Croucher, D., and Ranson, M. (2004) *Exp. Cell Res.* **297,** 259–271
8. Degryse, B., Neels, J. G., Czekay, R. P., Aertgeerts, K., Kamikubo, Y. I., and Loskutoff, D. J. (2004) *J. Biol. Chem.* **279,** 22595–22604
9. Huntington, J., Read, R., and Carrell, R. (2000) *Nature* **407,** 923–926
10. Saunders, D. N., Jankova, L., Harrop, S. J., Curmi, P. M. G., Gould, A. R., Ranson, M., and Baker, M. (2001) *J. Biol. Chem.* **276,** 43383–43389
11. Schmitt, M., Wilhelm, O., Reuning, U., Kruger, A., Harbeck, N., Lengyel, E., Graeff, H., Gansbacher, B., Kessler, H., and Burgle, M. (2000) *Fibrinolysis Proteolysis* **14,** 114–132
12. Duffy, M. J. (2004) *Curr. Pharm. Des.* **10,** 39–49
13. Ranson, M., and Andronicos, N. M. (2003) *Front. Biosci.* **8,** 294–304
14. Allen, B. J., Rizvi, S., Li, Y., Tian, Z., and Ranson, M. (2001) *Crit. Rev. Oncol. Hematol.* **39,** 39–146
15. Li, Y., Rizvi, S., Ranson, M., and Allen, B. J. (2002) *Br. J. Cancer.* **86,** 1197–1203
16. Ranson, M., Tian, Z., Andronicos, N. M., Rizvi, S., and Allen, B. J. (2002) *Breast Cancer Res. Treat.* **71,** 149–159
17. Allen, B. J., Tian, Z., Rizvi, S. M., Li, Y., and Ranson, M. (2003) *Br. J. Cancer.* **88,** 944–950
18. Moestrup, S. K., Nielsen, S., Andreasen, P., Jorgensen, K. E., Nykjaer, A., Roigaard, H., Gliemann, J., and Christensen, E. I. (1993) *J. Biol. Chem.* **268,** 16564–16570
19. Herz, J., Clouthier, D. E., and Hammer, R. E. (1992) *Cell* **71,** 411–421
20. Kounnas, M. Z., Henkin, J., Argraves, W. S., and Strickland, D. K. (1993) *J. Biol. Chem.* **268,** 21862–21867
21. Argraves, K. M., Battey, F. D., MacCalman, C. D., McCrae, K. R., Gafvels, M., Kozarsky, K. F., Chappell, D. A., Strauss, J. F., and Strickland, D. K. (1995) *J. Biol. Chem.* **270,** 26550–26557
22. Rettenberger, P. M., Oka, K., Ellgaard, L., Petersen, H. H., Christensen, A., Martensen, P. A., Monard, D., Etzerodt, M., Chan, L., and Andreasen, P. A. (1999) *J. Biol. Chem.* **274,** 8973–8980
23. Webb, D. J., Nguyen, D. H. D., Sankovic, M., and Gonias, S. L. (1999) *J. Biol. Chem.* **274,** 7412–7420
24. Stefansson, S., Kounnas, M. Z., Henkin, J., Mallampalli, R. K., Chappell, D. A., Strickland, D. K., and Argraves, W. S. (1995) *J. Cell Sci.* **108,** 2361–2368
25. Cubellis, M. V., Wun, T. C., and Blasi, F. (1990) *EMBO J.* **9,** 1079–1085
26. Jensen, P. H., Christensen, E. I., Ebbesen, P., Gliemann, J., and Andreasen, P. A. (1990) *Cell Regul.* **1,** 1043–1056
27. Nykjaer, A., Conese, M., Christensen, E. I., Olson, D., Cremona, O., Gliemann, J., and Blasi, F. (1997) *EMBO J.* **16,** 2610–2620
28. Moestrup, S. K., Kaltoft, K., Sottrup-Jensen, L., and Gliemann, J. (1990) *J. Biol. Chem.* **265,** 12623–12628
29. Nykjaer, A., Petersen, C. M., Moller, B., Jensen, P. H., Moestrup, S. K., Holtet, T. L., Etzerodt, M., Thogersen, H. C., Munch, M., and Andreasen, P. A. (1992) *J. Biol. Chem.* **267,** 14543–14546
30. Willnow, T. E., Goldstein, J. L., Orth, K., Brown, M. S., and Herz, J. (1992) *J. Biol. Chem.* **267,** 26172–26180
31. Knauer, M. F., Orlando, R. A., and Glabe, C. G. (1996) *Brain Res.* **740,** 6–14
32. Andreasen, P. A., Kjoller, L., Christensen, L., and Duffy, M. J. (1997) *Int. J. Cancer.* **72,** 1–22
33. Knauer, M. F., Hawley, S. B., and Knauer, D. J. (1997) *J. Biol. Chem.* **272,** 12261–12264
34. Gonias, S. L., Wu, L., and Salicioni, A. M. (2004) *Thromb. Haemostasis* **91,** 1056–1064
35. Strickland, D. K., Gonias, S. L., and Argraves, W. S. (2002) *Trends Endocrinol. Metab.* **13,** 66–74
36. Nykjaer, A., Kjoller, L., Cohen, R. L., Lawrence, D. A., Garni-Wagner, B. A., Todd, R. F., van Zonneveld, A. J., Gliemann, J., and Andreasen, P. A. (1994) *J. Biol. Chem.* **269,** 25668–25676
37. Rodenburg, K. W., Kjoller, L., Petersen, H. H., and Andreasen, P. A. (1998) *Biochem. J.* **329,** 55–63
38. Stefansson, S., Muhammad, S., Cheng, X. F., Battey, F. D., Strickland, D. K., and Lawrence, D. A. (1998) *J. Biol. Chem.* **273,** 6358–6366
39. Andersen, O. M., Petersen, H. H., Jacobsen, C., Moestrup, S. K., Etzerodt, M., Andreasen, P. A., and Thogersen, H. C. (2001) *Biochem. J.* **357,** 289–296
40. Heegaard, C. W., Simonsen, A. C. W., Oka, K., Kjoller, L., Christensen, A., Madsen, B., Ellgaard, L., Chan, L., and Andreasen, P. A. (1995) *J. Biol. Chem.* **270,** 20855–20861
41. Harrop, S. J., Jankova, L., Coles, M., Jardine, D., Whittaker, J. S., Gould, A. R., Meister, A., King, G. C., Mabbutt, B. C., and Curmi, P. M. G. (1999) *Structure* (*Lond.*) **7,** 43–54
42. Ranson, M., Andronicos, N. M., O'Mullane, M. J., and Baker, M. S. (1998) *Br. J. Cancer* **77,** 1586–1597
43. Andronicos, N. M., and Ranson, M. (2001) *Br. J. Cancer* **85,** 909–916
44. Misra, U. K., Gonzalez-Gronow, M., Gawdi, G., Hart, J. P., Johnson, C. E., and Pizzo, S. V. (2002) *J. Biol. Chem.* **277,** 42082–42087
45. Wang, S., Herndon, M. E., Ranganathan, S., Godyna, S., Lawler, J., Argraves, W. S., and Liau, G. (2004) *J. Cell. Biochem.* **91,** 766–776
46. Saunders, D. N., Buttigieg, K. M. L., Gould, A., McPhun, V., and Baker, M. S. (1998)

J. Biol. Chem. **273,** 10965–10971
47. Anderson, H. A., Chen, Y., and Norkin, L. C. (1996) *Mol. Cell. Biol.* **7,** 1825–1834
48. Boucher, P., Liu, P., Gotthardt, M., Hiesberger, T., Anderson, R. G. W., and Herz, J. (2002) *J. Biol. Chem.* **277,** 15507–15513
49. Wu, L., and Gonias, S. L. (2005) *J. Cell. Biochem.* **96,** 1021–1033
50. Stahl, A., and Mueller, B. M. (1995) *J. Cell Biol.* **129,** 335–344
51. Andreasen, P. A., Sottrup-Jensen, L., Kjoller, L., Nykjaer, A., Moestrup, S. K., Petersen, C. M., and Gliemann, J. (1994) *FEBS Lett.* **338,** 239–245
52. Zhang, J., Sakthivel, R., Kniss, D., Graham, C. H., Strickland, D. K., and McCrae, K. R. (1998) *J. Biol. Chem.* **273,** 32273–32280
53. Herz, J., and Strickland, D. K. (2001) *J. Clin. Investig.* **108,** 779–784
54. Webb, D. J., Thomas, K. S., and Gonias, S. L. (2001) *J. Cell Biol.* **152,** 741–751
55. Foekens, J. A., Buessecker, F., Peters, H. A., Krainick, U., van Putten, W. L., Look, M. P., Klijn, J. G., and Kramer, M. D. (1995) *Cancer Res.* **55,** 1423–1427
56. Czekay, R. P., Kuemmel, T. A., Orlanda, R. A., and Farquhar, M. G. (2001) *Mol. Biol. Cell* **12,** 1467–1479
57. Van Dam, E., ten Broeke, T., Jansen, K., Spijkers, P., and Stoorvogel, W. (2002) *J. Biol. Chem.* **277,** 48876–48883